Cite this: *Chem. Commun.*, 2012, **48**, 3812–3814

www.rsc.org/chemcomm

COMMUNICATION

# Design of an *in-house* ambient pressure AP-XPS using a bench-top X-ray source and the surface chemistry of ceria under reaction conditions†

**Franklin (Feng) Tao***

***Received 9th December 2011, Accepted 14th February 2012***
**DOI: 10.1039/c2cc17715c**

**A new *in-house* ambient pressure XPS (AP-XPS) was designed for the study of surfaces of materials under reaction conditions and during catalysis. Unique features of this in-house AP-XPS are the use of monochromated Al Kα and integration of a minimized reaction cell, and working conditions of up to 500 °C in gases of tens of Torr. Generation of oxygen vacancies on ceria and filling them with oxygen atoms were characterized *in operando*.**

In reactive environments (reactive gases or liquids), the surfaces of most materials are likely to restructure their geometric and electronic structure. Such changes have profound effects on the functions and properties of materials. In these cases, the structures and compositions of the material surfaces in a reactive environment in which they function are largely different than those characterized in high vacuum (HV) or ultrahigh vacuum (UHV), the operational environment of most conventional electron-based surface analytical techniques. The difference between the HV or UHV conditions of samples *during characterization* and the ambient or high pressure conditions of catalysts *during catalytic reactions* results in a gap in the study of heterogeneous catalysis, typically called a pressure gap. It is illustrated in Fig. 1. This difference was revealed by using *in situ* spectroscopy and microscopy.[1–4] One of the spectroscopic techniques is the synchrotron-based ambient pressure XPS,[1–3,5] which can examine catalyst surfaces up to a couple of Torr or so.

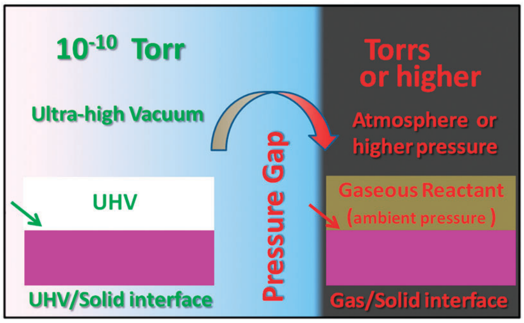

**Fig. 1** Schematic of the pressure gap in the study of heterogeneous catalysis.

Typically, the working conditions of heterogeneous catalysis are ambient or high temperature of catalysts in gaseous reactants at ambient or high pressure of reactants or liquid reactants.[6,7] The surface chemistry and structure of the as-synthesized catalysts vary during pretreatment, catalytic reactions, and deactivation. In addition, most of the heterogeneous catalysts are essentially nanoparticles of metals, oxides, carbides, *etc.*, and are particularly sensitive to reactive environments, such as oxidizing or reducing gases at high temperature.[1–3,7] Thus, the surface chemistry and structure of the nanocatalysts during catalysis could be different from those of as-synthesized catalysts before and/or after the catalysis. In some reactions a completely new phase is formed. For example, the active phase of Fischer–Tropsch synthesis, iron carbide, is formed on iron oxide at the beginning of the reaction at high temperatures.[8–10] A thermodynamic factor which drives the necessity of the study of surface structures and chemistry under reaction conditions is the pressure-dependent entropy contribution.[11] The magnitude of entropy contributed to the surface free energy *in ultrahigh vacuum* (*UHV*) is different *at ambient conditions*. The difference could be about 0.3 eV or even larger.[11] Thus, the pressure-dependent entropy could largely restructure the surface of a catalyst during catalysis.[12,13]

In some cases the surface structure and chemistry of an as-synthesized catalyst are the same as those during catalysis; in these cases the *ex situ* studies can represent information obtained during the reaction. However, it is expected that catalyst surfaces under reaction conditions could be different in contrast to those before reactions for many reactions. This is demonstrated in the recent studies.[3,4,9–12,14–22] Thus, the investigation of the chemistry of catalyst surfaces under reaction conditions, called *operando* study, is crucial for understanding catalytic mechanisms and providing insight into the design of new catalysts. *Operando studies* in this communication are defined as the *studies under reaction conditions or during reactions*.

A synchrotron-based AP-XPS obtained at a Torr pressure range was developed at Advanced Light Sources.[23] Later on a couple of synchrotron-based AP-XPS systems were built by using synchrotron radiations to excite electrons from sub-shells.[24,25] Gases were introduced and remained in a chamber with a volume of a few litres. This reaction chamber was installed into the AP-XPS system. The access is granted on the basis of proposal review due to the nature of public facilities and expensive maintenance. An alternative solution is the design of an *in-house* ambient pressure XPS using affordable *bench top* X-ray sources

---

*Department of Chemistry and Biochemistry, University of Notre Dame, Notre Dame, IN 46556, USA. E-mail: ftao@nd.edu*

† Electronic supplementary information (ESI) available. See DOI: 10.1039/c2cc17715c

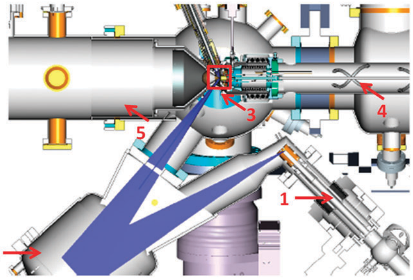

**Fig. 2** In-house X-ray source, Al Kα for the excitation of photoelectrons from catalysts in the gaseous environment of the reaction cell. 1: electron gun; 2: monochromator of Al Kα; 3: reaction cell; 4: manipulator of the reaction cell; 5: differential pumping stages connected to the energy analyzer.

such as Al Kα. The term "*in-house*" refers to the feature that the *in-house* AP-XPS uses X-rays generated from an X-ray gun which is affordable by any research groups. Here the successful design of an *in-house* AP-XPS with a working pressure of 25–50 Torr, near ambient pressure, is reported. As shown in Fig. 2, the Al Kα is used as the X-ray source of our *in-house* AP-XPS. X-Rays are generated from an X-ray gun (XR50, Specs Surface Nano Analysis GmbH). A monochromator (XRF 1000MC, Specs Surface Nano Analysis GmbH) is used to focus the X-ray beam.

The AP-XPS analytical chamber has a monochromated X-ray source described above, a minimized reaction cell for *operando* study of catalysts in a flowing mode, a differential pumping system conducted to an electrostatic hemisphere energy analyzer, and a mass spectrometer for analysis of the gas composition of the reaction cell. The reaction cell is the core part designed for carrying out reactions on catalysts at ambient or high temperature in reactant gases with certain pressures and allowing the energy analyzer to collect photoelectrons excited from the catalyst surface.

A manipulator was installed in the AP-XPS analytical chamber to manipulate the position of the reaction cell (4 in Fig. 2 and Fig. 3a). This reaction cell was assembled at the end of the manipulator (Fig. 3a). The reaction cell has four windows for transmitting monochromated X-ray to the sample surface, brightening the sample and the nozzle in the reaction cell for video recording, watching the sample and the aperture through a video camera, and a port for the second X-ray source or other applications.

A nozzle with an aperture of 300 μm was assembled at the end of the reaction cell (Fig. 3b). It is engaged to the pre-lens through a manipulator during *operando* studies. The aperture of the nozzle (marked on Fig. 3b) allows photoelectrons to escape from the reaction cell to be collected by the energy analyzer. It was minimized so that a good vacuum can be obtained at the pre-lens from where photoelectrons are conducted to lenses of the energy analyzer. The sample stage (the part to accommodate the sample holder) was assembled near the aperture but kept at a distance of 0.3 mm. This distance is similar to the inelastic mean free path (IMFP) of photoelectrons of 500 eV in gaseous phase with a pressure of about tens of Torr.[26]

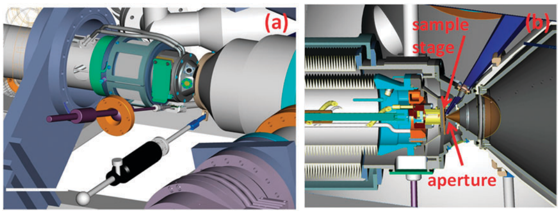

**Fig. 3** Reaction cell for *operando* studies. (a) External view of the reaction cell installed at the end of the sample manipulator; (b) section view of this reaction cell. (Detailed information is available in ESI†.)

This *in-house* AP-XPS uses a hemispheric energy analyzer purchased from Specs Nano and Surface Analysis GmbH. Three differential pumping stages were installed between the reaction cell and the energy analyzer (see ESI†). The aperture mounted on the reaction cell separates the high pressure environment of the reaction cell from the vacuum of the first differential pumping stage. A quadrupole mass spectrometer is mounted at the third differential pumping stage for the gas analyses. The gases leaked naturally from the reaction cell through the aperture and are analyzed by the mass spectrometer. Such an on-line analysis of gas composition (reactants and products) allows for building a simultaneous correlation between the products and the surface chemistry of catalysts examined with AP-XPS. This simultaneous measurement of products provides the opportunity to build an intrinsic correlation between the surface chemistry of catalysts *in operando* and their catalytic performance. Such a correlation will provide critical insight for understanding catalysis and designing catalysts.

By using this in-house AP-XPS we examined the Ag(111) surface in $N_2$ with different pressures. The photoemission features of Ag3d of an Ag(111) single crystal and N1s in the reaction cell were acquired. Fig. 4 presents the Ag3d and N1s peaks at different pressures of $N_2$. At a pressure of $10^{-8}$ Torr, $N_2$ does not adsorb on Ag(111). There is not any nitrogen molecule adsorbed on Ag(111) at room temperature or above in the whole pressure range ($10^{-10}$–50 Torr). In 1 Torr of $N_2$, both Ag3d and N1s features from $N_2$ in gaseous phase are very clear. Notably, the peak position of the N1s photoemission peak is about 406 eV instead of 399.5 eV of N1s in a species adsorbed on the surface. The different binding energy of gas phases, typically a few eV higher than that of adsorbed molecules, actually offers us an opportunity to identify gaseous phases such as products of catalysis. With the increase of the $N_2$ pressure, the ratio of counts of N1s to Ag3d is increased. Their absolute counts are decreased due to larger gas density at a higher pressure. At a pressure of 25 Torr (Fig. 4b), both Ag3d and N1s photoemission features were clearly identified.

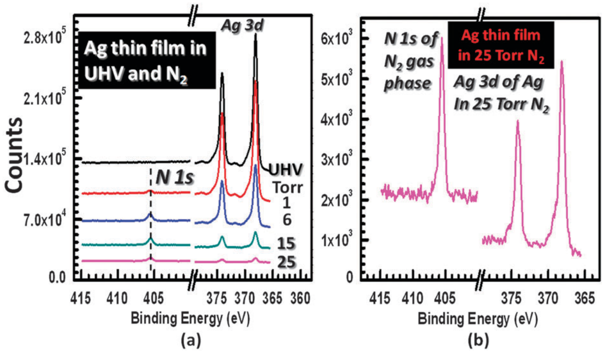

**Fig. 4** (a) XPS spectra of Ag3d and N1s collected from Ag(111) in UHV and in different pressures of $N_2$. (b) Enlargement of the Ag3d and N1s spectra collected at 25 Torr of $N_2$.

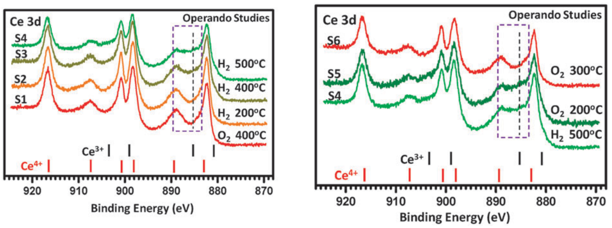

**Fig. 5** Evolution of Ce3d XPS spectra of $CeO_2$ under different reaction conditions as listed. The lines below the spectra mark the peak positions of pure $Ce_2O_3$ and $CeO_2$, respectively.[28] S1, S2, S3, S4, S5, and S6 in the figure mark the sequence of experimental steps.

The distance between the Ag(111) surface and the aperture is 0.3 mm. This distance allows an efficient collection of photoelectrons from sample surfaces at 25–50 Torr $N_2$. As the mean free path is basically reversely proportional to the density of gas phase, a distance of 20 μm is necessary for an efficient collection of photoelectrons from a sample surface in gas of 760 Torr. Moving a sample to an aperture from a visible distance (~1 mm) to the requested distance (20 μm) is challenging even if a digitalized mechanic motor is used. But it can be done readily by a digitalized mechanic motor for coarse approach together with a piezoelectric motor for precise approach such as a piezo motor used in some STM systems.[27] My group at Notre Dame is testing this idea of mine.

Ceria is one of the most important reducible oxides widely used in heterogeneous catalysis. It is well known that surface oxygen vacancies on a $CeO_2$ surface are active sites for dissociative or molecular adsorption during catalysis. For example, oxygen vacancies dissociate oxygen molecules during CO oxidation in three-way catalysts and water molecules in water-gas shift.[29] The surface chemistry of $CeO_2$ in an $O_2$ environment in a flowing reactor was examined with this in-house AP-XPS. Fig. 5 presents the Ce3d XPS spectra acquired under different reaction conditions. The spectra obtained in UHV at room temperature (not shown) have a small number of oxygen vacancies. During annealing of the samples at 400 °C in $O_2$, the fraction of $Ce^{3+}$ is decreased. Most of the cerium atoms exist in the form of $Ce^{4+}$. Once the sample is cooled to 100 °C and oxygen is purged, $H_2$ is introduced. Ce3d spectra were collected during annealing in $H_2$ to different temperatures. The deconvoluted data showed the decrease of the fraction of $Ce^{4+}$, suggesting the reduction of $Ce^{4+}$ by $H_2$ and the generation of oxygen vacancies. The on-line mass spectrometer identified the desorbed $H_2O$ molecules due to the reaction of surface lattice oxide with $H_2$. The AP-XPS studies confirmed the capability of refilling the generated oxygen vacancies using $O_2$. Upon purging hydrogen and then filling oxygen, the $Ce^{4+}$ is partially reduced to $Ce^{3+}$.

The *operando* studies of $CeO_2$ thin films under reaction conditions clearly provided the dynamic nature of the $CeO_2$ surface under different reaction conditions. Furthermore, the deconvoluted data can be used to calculate the enthalpy of reduction and oxidation of the $CeO_2$ surface. The enthalpy of different oxides will help clarify the role of these sites in catalysis.

In summary, an *in-house* ambient pressure X-ray photoelectron spectroscopy (AP-XPS) was successfully designed. This *in-house* AP-XPS uses affordable *bench top* monochromated Al Kα instead of synchrotron facilities. This design has made the AP-XPS technique available daily for any individual research group. A new chamber-in-chamber reaction cell with a minimized volume of gaseous reactants, 15 ml, allows the study of catalytic kinetics. This *in-house* AP-XPS can characterize the surface chemistry of materials at 120–773 K in a pressure range of $1 \times 10^{-10}$ to 25–50 Torr. The oxidation and reduction of ceria were monitored in operando.

F.T. acknowledges the help from Specs Surface Nano Analysis GmbH and financial support from University of Notre Dame and U. S. Department of Energy.

## Notes and references

1 F. Tao, M. E. Grass, Y. Zhang, D. R. Butcher, J. R. Renzas, Z. Liu, J. Y. Chung, B. S. Mun, M. Salmeron and G. A. Somorjai, *Science*, 2008, **322**, 932–934.
2 F. Tao, S. Dag, L.-W. Wang, Z. Liu, D. R. Butcher, H. Bluhm, M. Salmeron and G. A. Somorjai, *Science*, 2010, **327**, 850–853.
3 F. Tao and M. Salmeron, *Science*, 2011, **331**, 171–174.
4 M. S. Altman, *Science*, 2010, **327**, 789–790.
5 F. Tao, S. Dag, L.-W. Wang, Z. Liu, D. R. Butcher, M. Salmeron and G. A. Somorjai, *Nano Lett.*, 2009, **9**, 2167–2171.
6 G. A. Somorjai and Y. Li, *Introduction to surface chemistry and catalysis*, Wiley, Hoboken, N.J., 2010.
7 G. Ertl, H. Knoözinger and J. Weitkamp, *Handbook of heterogeneous catalysis*, VCH, Weinheim, 1997.
8 E. de Smit and B. M. Weckhuysen, *Chem. Soc. Rev.*, 2008, **37**, 2758–2781.
9 F. M. F. de Groot, E. de Smit, I. Swart, J. F. Creemer, G. H. Hoveling, M. K. Gilles, T. Tyliszczak, P. J. Kooyman, H. W. Zandbergen, C. Morin and B. M. Weckhuysen, *Nature*, 2008, **456**, U222–U239.
10 E. de Smit, M. M. van Schooneveld, F. Cinquini, H. Bluhm, P. Sautet, F. M. F. de Groot and B. M. Weckhuysen, *Angew. Chem., Int. Ed.*, 2011, **50**, 1584–1588.
11 M. Salmeron and R. Schlogl, *Surf. Sci. Rep.*, 2008, **63**, 169–199.
12 F. Tao, S. Dag, L. W. Wang, Z. Liu, D. R. Butcher, H. Bluhm, M. Salmeron and G. A. Somorjai, *Science*, 2010, **327**, 850–853.
13 G. Ketteler, D. F. Ogletree, H. Bluhm, H. J. Liu, E. L. D. Hebenstreit and M. Salmeron, *J. Am. Chem. Soc.*, 2005, **127**, 18269–18273.
14 G. A. Somorjai, F. Tao and J. Y. Park, *Top. Catal.*, 2008, **47**, 1–14.
15 F. Tao, M. E. Grass, Y. W. Zhang, D. R. Butcher, J. R. Renzas, Z. Liu, J. Y. Chung, B. S. Mun, M. Salmeron and G. A. Somorjai, *Science*, 2008, **322**, 932–934.
16 A. M. Beale, S. D. M. Jacques and B. M. Weckhuysen, *Chem. Soc. Rev.*, 2010, **39**, 4656–4672.
17 S. M. Bennici, B. M. Vogelaar, T. A. Nijhuis and B. M. Weckhuysen, *Angew. Chem., Int. Ed.*, 2007, **46**, 5412–5416.
18 P. L. Hansen, J. B. Wagner, S. Helveg, J. R. Rostrup-Nielsen, B. S. Clausen and H. Topsoe, *Science*, 2002, **295**, 2053–2055.
19 T. W. Hansen, J. B. Wagner, P. L. Hansen, S. Dahl, H. Topsoe and C. J. H. Jacobsen, *Science*, 2001, **294**, 1508–1510.
20 S. J. Tinnemans, M. H. F. Kox, T. A. Nijhuis, T. Visser and B. M. Weckhuysen, *Phys. Chem. Chem. Phys.*, 2005, **7**, 211–216.
21 S. J. Tinnemans, J. G. Mesu, K. Kervinen, T. Visser, T. A. Nijhuis, A. M. Beale, D. E. Keller, A. M. J. van der Eerden and B. M. Weckhuysen, *Catal. Today*, 2006, **113**, 3–15.
22 E. Stavitski and B. M. Weckhuysen, *Chem. Soc. Rev.*, 2010, **39**, 4615–4625.
23 D. F. Ogletree, H. Bluhm, G. Lebedev, C. S. Fadley, Z. Hussain and M. Salmeron, *Rev. Sci. Instrum.*, 2002, **73**, 3872–3877.
24 D. F. Ogletree, H. Bluhm, E. D. Hebenstreit and M. Salmeron, *Nucl. Instrum. Methods Phys. Res., Sect. A* 2009, **601**, 151–160.
25 M. E. Grass, P. G. Karlsson, F. Aksoy, M. Lundqvist, B. Wannberg, B. S. Mun, Z. Hussain and Z. Liu, *Rev. Sci. Instrum.*, 2010, **81**, 053106.
26 NIST Standard Reference Database 71, (2000), Version 1.1.
27 F. Tao, D. Tang, M. Salmeron and G. A. Somorjai, *Rev. Sci. Instrum.*, 2008, **79**, 084101.
28 D. R. Mullins, S. H. Overbury and D. R. Huntley, *Surf. Sci.*, 1998, **409**, 307–319.
29 J. A. Rodriguez, S. Ma, P. Liu, J. Hrbek, J. Evans and M. Perez, *Science*, 2007, **318**, 1757–1760.